INTERNATIONAL JOURNAL OF REMOTE SENSING, 2017
VOL. 38, NO. 7, 1912–1939
http://dx.doi.org/10.1080/01431161.2016.1230288

Taylor & Francis
Taylor & Francis Group

Insuring forage through satellites: testing alternative indices against grassland production estimates for France

Antoine Roumiguié[a], Grégoire Sigel[b], Hervé Poilvé[b], Bruno Bouchard[c], Anton Vrieling[d] and Anne Jacquin[a]

[a]Institut National Polytechnique de Toulouse, Université de Toulouse, Ecole d'Ingénieurs de Purpan, UMR 1201 DYNAFOR, Toulouse, France; [b]Airbus Defence and Space, Toulouse, France; [c]CEREMADE, Université Paris Dauphine, Paris, France; [d]Faculty of Geo-Information Science and Earth Observation, University of Twente, Enschede, The Netherlands

ABSTRACT

To mitigate impacts of climate-related reduced productivity of French grasslands, a new insurance scheme bases indemnity payouts to farmers on a Moderate Resolution Imaging Spectroradiometer (MODIS)-derived forage production index (FPI). The objective of this study is to compare several approaches for deriving FPI from satellite data to assess whether better relationships with forage productivity can be attained. The approaches assess pasture productivity using as five input factors estimated from remote sensing and ancillary data, i.e.: (1) fraction of absorbed photosynthetically active radiation (*f*APAR); (2) radiation use efficiency estimates; (3) PAR estimates; (4) leaf senescence modelling; and (5) growing season modelling . All the possible combinations from these five factors, including different modalities to estimate some of them, lead to 768 models. Model outputs are compared to reference grassland production estimates provided by a mechanistic model (Information et Suivi Objectif des Prairies – ISOP – system) for a sample of 25 forage regions across France for the years 2003, 2007, 2009, 2011, and 2012 (containing one humid, two normal, and two dry years). Results revealed that: (1) the baseline model based on the fraction of green vegetation cover (*f*Cover) seasonal integral has a reasonable linear relationship to production estimates (standardized root mean square error – SRMSE = 0.57 and coefficient of determination – R^2 = 0.68); (2) performance of the baseline model improved with a quadratic function (SRMSE = 0.54 and R^2 = 0.71); (3) 34 models outperform the baseline model. We, therefore, suggest to replace the baseline model with the best-performing model (SRMSE = 0.42 and R^2 = 0.83) in the insurance product. This model integrates daily *f*Cover with a water stress index and sums these over a variable monitoring period in space and time characterized by the phenological indicators start of season and end of season derived from the *f*Cover annual profile.

ARTICLE HISTORY
Received 17 December 2015
Accepted 22 August 2016

CONTACT Antoine Roumiguié antoine.roumiguie@purpan.fr Institut National Polytechnique de Toulouse, Université de Toulouse, Ecole d'Ingénieurs de Purpan, UMR 1201 DYNAFOR, Toulouse, France

1. Introduction

Grasslands are a key resource for livestock production. Animal breeders adjust the size of their flocks and manage them based on an expected production potential. However, drought can cause significant declines in grassland production (Boyer 2008; Mosnier, Fourdin et al. 2014). Such events may force producers to look for alternative feed sources on the market in order to face the constant demand by livestock and to prevent economic losses or animal illnesses/deaths (Lemaire, Micol et al. 2006; Veysset, Bebin, and Lherm 2007; Mosnier, Agabriel et al. 2008). Among existing solutions to limit the impact of a loss in biomass production, insurance is interesting because it provides the insured with an opportunity to buy additional animal feed and withstand the temporary crisis (Noury, Fourdin, and Pauthenet 2013). However, traditional insurance policies based on farm-based assessment of losses are impractical due to the difficulty of estimating annual grassland production for insured individuals given that mowing and grazing are common practices during the year (de Leeuw, Vrieling et al. 2014). It is a challenge to propose a marketable forage insurance product that effectively accounts for the annual variability in production and that can reach scale. Unlike traditional insurance schemes that assess losses on an individual basis, index-based insurance (IBI) offers payouts based on a biophysical index which triggers a payment to all insured farmers within a geographically-defined space (Ceccato, Brown et al. 2008; Hazell and Hess 2010). Remotely-sensed time series provided by medium resolution sensors have the potential to monitor vegetation over large areas at a spatial resolution (approximately 250 m) matching the scale of grassland fields and with good acquisition frequencies (Lu 2006; Cai, Yuan et al. 2014; Jin, Yang et al. 2014). The main challenge for IBI is to minimize the basis risk, i.e. the situation where farmers do not get paid during production shortfalls, or get paid when not facing losses. This requires that the index correlates well with real losses experienced by the insured (Hellmuth, Osgood et al. 2009; Sandmark, Debar, and Tatin-Jaleran 2013). Grassland productivity estimates are currently derived from

(1) mechanistic approaches, i.e. models that describe the physiological mechanisms of grassland and their interaction with abiotic factors;
(2) semi-empirical approaches that simulate physiological processes with simpler equations than mechanistic models and with a limited number of data and mechanisms (Potter, Randerson et al. 1993; Field, Randerson, and Malmström 1995; Veroustraete, Sabbe, and Eerens 2002; Seaquist, Olsson, and Ardö 2003; Maselli, Argenti et al. 2013; Rembold, Atzberger et al. 2013; Gilabert, Moreno et al. 2015);
(3) empirical approaches (Delécolle, Maas et al. 1992) that use simple models based only on field measurements (Jouven, Carrère, and Baumont 2006) or remote-sensing indices (Meroni, Marinho et al. 2013).

Mechanistic approaches are normally applied to small areas with homogeneous conditions, but can be aggregated to generate productivity estimates at larger scales (Di Bella, Faivre et al. 2004; Courault, Hadria et al. 2010). Nonetheless, due to their high data demand, mechanistic approaches are cumbersome to implement at a national scale with

complex spatial heterogeneity. Empirical approaches using models based on field measurement of grassland productivity are also difficult to implement because they are expensive, time-consuming and labour intensive (Maselli, Papale et al. 2009). In light of these weaknesses, remote-sensing technology can fill a gap by contributing to effective biomass estimation over larger regions (Gaitán, Bran et al. 2013; Gao, Xu et al. 2013). Many remote-sensing approaches are based on a simple empirical relationship between a remote-sensing index and biomass production, require significantly less data as compared to mechanistic models, and are effective for monitoring large production areas (Running, Nemani et al. 2004; Xu, Yang et al. 2007; Jin, Yang et al. 2014; Meroni, Rembold et al. 2014, Meroni, Verstraete et al. 2014; Dusseux, Hubert-Moy et al. 2015) . However, given their empirical nature, these remote-sensing approaches need to be calibrated for local conditions (Meroni, Marinho et al. 2013).

To address the limitations of mechanistic or empirical approaches, production efficiency models (PEMs) have emerged (for a detailed review, see McCallum, Wagner et al. 2009). Also referred to as light use efficiency (LUE) models, they rely on the relationship between the meteorological constraint of available sunlight reaching the vegetation and the ecological constraint of the amount of leaf area available to absorb that solar energy (Running, Baldochhi et al. 1999). PEMs require as input data on environmental variables, including solar radiation, air temperature, water availability, and vegetation conditions. The basic consideration underlying these models is that the estimation of grassland biomass production over large areas (e.g. nation scale) can reach better precision by suitably integrating multiple sources of remote sensing and ancillary data (Seaquist, Olsson, and Ardö 2003; Launay and Guerif 2005; Maselli, Papale et al. 2009).

Presently, the predominant method to develop index-based insurance for grasslands is to use an empirical approach with a vegetation index derived from satellite data to estimate biomass production. We present some examples of operational products in Table 1.

Among the eight products, six use vegetation indices and, for five, it is the normalized difference vegetation index (NDVI) (Rouse, Hass et al. 1974). The reasons for using NDVI likely include data accessibility, the spatial, and temporal resolutions offered by coarse and moderate instruments, and the stronger relationship between NDVI and biomass production (Huete, Didan et al. 2002; Wang, Adiku et al. 2005) as compared to what is typically observed between rainfall indices and biomass (Barnett and Mahul 2007; Hazell and Hess 2010; Rao 2010; Sandmark, Debar, and Tatin-Jaleran 2013).

In France, since the beginning of the 2000s, grassland damage from drought events is estimated regionally with a mechanistic approach (Ruget, Novak, and Granger 2006). In 2015, Crédit Agricole Assurances Pacifica (Pacifica), associated with Airbus Defence & Space (Airbus D&S), proposed an index-based insurance solution to assess local grassland production losses (Geeraert 2012; Crédit Agricole 2013; Bergeot 2015). They developed an indicator called the forage production index (FPI) that empirically estimates and monitors in near real-time grassland biomass production in France. Rather than NDVI, the indicator uses the fraction of green vegetation cover (*f*Cover), which behaves similar as the common remote-sensing parameter fraction of absorbed photosynthetically active radiation (*f*APAR) (Baret, Weiss et al. 2005). Derived from radiative transfer models, *f*Cover is a biophysical parameter that can overcome limitations of empirical vegetation indices such as the NDVI: dependency on data processing level (raw, calibrated, reflectance) and sensors sources; saturation effect;

Table 1. Description of the main characteristics of some operational index-based insurances for grassland in the World (based on Agroasemex 2006; Agroseguro 2012; Risk Management Agency 2013, Agriculture Financial Services Corporation 2014).

Country	Index	Input data source	Geographical scale of biomass estimation	Approach for biomass estimation
Spain	NDVI	MODIS 250 m 10 days	County (*Comarcas*)	Empirical model Comparison of historical and actual decade NDVI values
Mexico	NDVI	NOAA-AVHRR 1.1 km Daily	Farm reference	Empirical model Annual sum of NDVI of previous year integrating livestock management data of year *n*
USA	NDVI	USG-EROS 8 km Daily	County	Empirical model Comparison of historical and actual mean NDVI values over a defined period
USA	Rainfall	NOAA CPC Weather station Daily	Grid of 27 km	Empirical model Comparison of historical and actual daily rainfall over 2 months period
Canada Alberta	NDVI	NOAA-AVHRR 1.1 km 8 days	County	Empirical model Comparison of historical and actual NDVI weekly values
Canada Ontario	Rainfall	Weather station Daily	Weather station distribution	Empirical model Comparison of historical and actual sum of rainfall over a defined period
France	*f*Cover	MODIS/MERIS 300 m 10 days	County	Empirical model Comparison of historical and actual sum of daily *f*Cover between 1 February and 31 October
France	Biomass production	Climatic data Daily Soil and field data (constant)	Forage region	Mechanistic model Comparison of historical and actual annual production

sensitivity to cloud veils, soil colour, and presence of non-photosynthetic vegetation (Asner, Wessman, and Archer 1998; Running, Nemani et al. 2004; Camacho and Torralba 2010; Camacho and Cernicharo 2011). In a previous study (Roumiguié, Jacquin, Sigel, Poilve, Hagolle, et al. 2015), a direct comparison between *in situ* grassland biomass measurements and FPI derived from *f*Cover measured with high resolution (HR) time series was conducted. Recently, a complementary validation study was conducted with a bottom–up approach (combining field, high, and medium spatial resolution scales) for validating the use of an annual FPI as a surrogate for inter-annual biomass variation at a 1 km resolution (Roumiguié, Jacquin, Sigel, Poilve, Lepoivre, et al. 2015). Results showed that FPI could be used as a proxy to monitor annual biomass production of grasslands and its variations with a satisfactory level of error (root mean square error – RMSE = 14.5 %). However, this level also indicates that there may be scope for improvement.

The objective of this article is to evaluate if semi-empirical approaches based on PEM can provide more accurate grassland biomass estimates than the *f*Cover-based FPI currently used in the French insurance product. This analysis should result in promising avenues for further improvement of the forage production index.

2. Models to assess forage production

2.1. *Baseline model*

The empirical baseline model was described by Roumiguié, Jacquin, Sigel, Poilve, Hagolle, et al. (2015) and can be written in the following form:

$$\mathrm{FPI}_n = \sum_{i=\mathrm{SOS}}^{\mathrm{EOS}} (f\mathrm{Cover\ Grassland})_i - (\mathrm{NPV})_i, \tag{1}$$

where SOS and EOS are start of season and end of season. For the baseline model, these are fixed at, respectively, 1 February and 31 October. For any year *n*, the model sums the daily grassland *f*Cover between 1 February and 31 October ($f\mathrm{Cover\ Grassland}_i$) while simultaneously subtracting the proportion of non-productive vegetation (NPV). This parameter represents the biomass that could not be harvested. It is an empirical value, fixed in time and variable across space, based on statistical grassland biomass production data provided by the French Ministry of Agriculture at the administrative department scale.

2.2. *New models*

2.2.1. *Theoretical basis*

The new models are based on the PEM (Monteith and Moss 1977), which estimates daily gross primary productivity (P_i) as follows:

$$P_i = (\mathrm{RUE})_i \times (\mathrm{PAR})_i \times (f\mathrm{APAR})_i, \tag{2}$$

where RUE_i is the daily radiation use efficiency, $f\mathrm{APAR}_i$ is the daily fraction of photosynthetic active radiation and PAR_i is the daily photosynthetic active radiation.

Annual biomass production (B_n), integrating the leaf senescence function D_i, and the growing season characteristics, is computed in Equation (3).

$$B_n = \sum_{m=1}^{M} \left(\sum_{i=(\mathrm{SOS})_m}^{(\mathrm{EOS})_m} P_{m,i} - D_{m,i} \right), \tag{3}$$

where m is the number of phenological cycles within the year, D_i is the function that simulates leaf senescence during vegetative growth based on leaf life span (l), SOS and EOS are the two phenological indicators used to determine SOS and EOS.

2.2.2. *Factor description*

*f*APAR $_i$ describes the fraction of the total received photosynthetically active radiation that is absorbed by the vegetation. It can be directly estimated from optical remote-sensing data through radiative transfer models or through empirical relationships with vegetation indices. In our study, we considered two biophysical parameters: *f*Cover is the one currently used to calculate FPI and *f*APAR is the traditional parameter prescribed to implement PEM (Monteith and Moss 1977; McCallum, Wagner et al. 2009); and one vegetation index, i.e. the NDVI.

The grassland RUE_i is defined as the ratio between the above-ground dry matter and the absorbed radiation following defoliation (Duru, Adam et al. 2009). In our study, RUE_i is modelled by the following equation:

$$\mathrm{RUE}_i = T_i \times S_i \times G_i \times W_i, \tag{4}$$

where T_i, S_i, G_i, and W_i are efficiency-reducing factor for temperature, season, phenology, and water stress, respectively. The effect of nutrient availability is not estimated, as recommended by Duru, Adam et al. (2009) and Cros, Duru et al. (2003), due to lack of data. Season and phenology effect corresponds to the modification of assimilates allocation between aerial biomass and root during vegetative growth. The first three factors can be modelled (Cai, Yuan et al. 2014):

$$T_i = 0.037 + 0.09 \times t_i - 0.0022 \times t_i^2, \tag{5}$$

where t_i is the daily mean temperature in °C;

$$S_i = \frac{-0.6j}{180} + 2.5 + 32\left(\frac{0.6}{180}\right), \tag{6}$$

where j is the number of days from 1 January to day i;

$$G_i = \begin{cases} 1, if\ d_i < l \\ \left(-2.9 \times 10^{-6}\right) d_i^2 + \left(6.27 \times 10^{-3}\right) d_i - 1.88, if\ l \le d_i < 2l \\ 0.64, if\ d_i \ge 2l \end{cases}, \tag{7}$$

where l is equal to 700°C according to Duru, Adam et al. (2009) giving a range between 500°C and 800°C depending on the species and d_i is the daily degree-day in °C.

W_i can be estimated from the ratio between actual and potential evapotranspiration (Maselli, Papale et al. 2009, Maselli, Argenti et al. 2013). Maselli, Papale et al. (2009) proposed this specific index to improve biomass estimation in arid and semi-arid regions. Vegetation index and biophysical parameters, such as NDVI, *f*Cover, or *f*APAR are sensitive to long duration water limitation because optical remote-sensing data can detect changes in canopy structure and defoliation. However, these data do not catch brief water shortages

that could induce a decrease in the RUE. W_i is interesting to observe during drought situations as it requires only a limited number of climatic data (temperature, rainfall, and radiation).

$$W_i = \begin{cases} 0.5 + 0.5\frac{a_i}{e_i}, if\ a_i < e_i \\ 1, if\ a_i > e_i \end{cases}, \tag{8}$$

where a_i is the daily actual evapotranspiration and e_i is the daily potential evapotranspiration.

PAR_i is estimated with Equation (9) as a proportion of the daily solar radiation (r_i) according to Gilabert, Moreno et al. (2015) with a value of 48 % based on Gosse, Varlet-Grancher et al. (1986):

$$PAR_i = 0.48 \times r_i. \tag{9}$$

The proportion of senescent vegetation in the production estimate is determined by modelling leaf senescence (D_i) presented in Equation (10). Until the time the first cohort of leaves begin to senesce ($d_i < l$), we assumed that no senescent material is present. For the following cohort of leaves ($d_i > l$), the senescent material of day i depends on the daily biomass production at the day of emergence of these new leaves ($P_{d_i - l}$), modified with a senescence rate calculated according to the daily mean temperature (t_i), the leaf-life span (l), and a constant coefficient of remobilization ($\gamma = 0.15$) corresponding to the fraction of senescent biomass reallocated in green matter (Duru, Adam et al. 2009, Duru, Cruz et al. 2010). The importance to integrate the contribution of leaf senescence in the production model was addressed by Duru, Adam et al. (2009):

$$D_i = \begin{cases} 0, \text{if } d_i < l \\ (1-\gamma) \times P_{(d_i - l)} \times \frac{t_i}{l}, \text{if } d_i > l \end{cases}, \tag{10}$$

where l is equal to 700°C according Duru, Adam et al. (2009) giving a range between 500°C and 800°C depending on the species, t_i is the daily mean temperature in °C, and d_i is the daily degree-day in °C (see Section 3.3 for definition of equations).

Richardson, Keenan et al. (2013) demonstrated the ability of phenological indicators to be used as proxy to monitor climatic and environmental effects on grassland phenology. They concluded the necessity to consider those indicators characterizing vegetation growth while estimating vegetation productivity. Figure 1 illustrates the phenology variability of grasslands in five forage regions (FRs), represented by a mean *f*Cover profile observed between 2003 and 2012, which shows that several locations have a double growing cycle due to their specific climatic conditions.

In this work, growing season characteristics are addressed by introducing two modalities in Equation (3) to calculate annual biomass production (B_n), i.e. (a) the monitoring period defined by two phenological indicators, the SOS and the EOS, and (b) the number of phenological cycles (m) of grassland within a year.

For the developed models, the modalities SOS/EOS and m can present variable values. Regarding SOS/EOS, the values can be fixed as in the baseline model or made spatially and temporally variable according to the grassland growth cycle. In our study, they are determined annually at the FR scale from the analysis of the *f*Cover time series. For m, it can be adjusted to simulate a uni- ($m = 1$) or bi-modal ($m = 2$) seasonality for

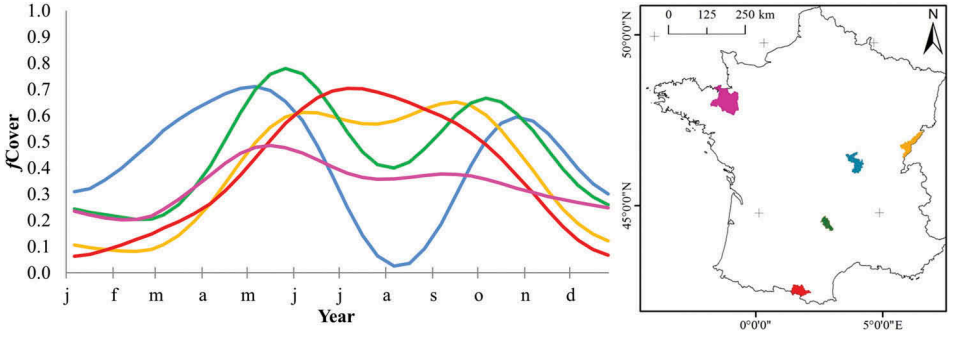

Figure 1. Grassland phenology variability in five forage regions. Curves correspond to the mean *f*Cover observed between 2003 and 2012. Colours of the curves allow identifying the corresponding forage region on the map.

the grassland within the year. The interest of such a modification is to consider the annual biomass production (B_n) as the result of one or two growing cycles. Choosing a bi-modal seasonality has an influence on the growing degrees day (d_i) and on the SOS/EOS values.

3. Materials and methods

3.1. *Application site*

Hentgen (1982) divided France into 229 homogeneous agro-climatic regions, or Forage Regions (FR), having similar grassland production potential. The study sites here are composed of various FRs with one FR representing one spatial unit for the model validation. A sample of 25 FRs is selected using the same criteria as in Di Bella, Faivre et al. (2004) (altitude, grassland percentage, temperature, and rainfall) in order to represent areas with different climatic situations. Figure 2 illustrates the site condition variability of these FRs. The grassland percentage represents the surface classified as grassland cover, according to the land-cover classification rules of the FPI processing chain (Roumiguié, Jacquin, Sigel, Poilve, Lepoivre, et al. 2015), divided by the total area of the FR. Temperature and rainfall variables correspond, respectively, to the temperature and the annual cumulated rainfall averaged over 10 years (2003–2012).

For model validation, five years representing specific climatic situations are selected. Figure 3 shows the annual, spring, and summer rainfall and temperature variations for the five selected years compared to a historical reference (2003–2012) observed in the 25 FRs. Drought conditions in France during 2003 and 2011 are prominent. In 2003, drought affected vegetation during spring and summer with elevated summer temperatures. In 2011, water scarcity and hot temperatures were only observed during the spring. Figure 3 also points out abundant rainfall and hot temperatures in spring suitable for forage production in 2007. Finally, 2009 and 2012 represent normal climatic years for the study sites.

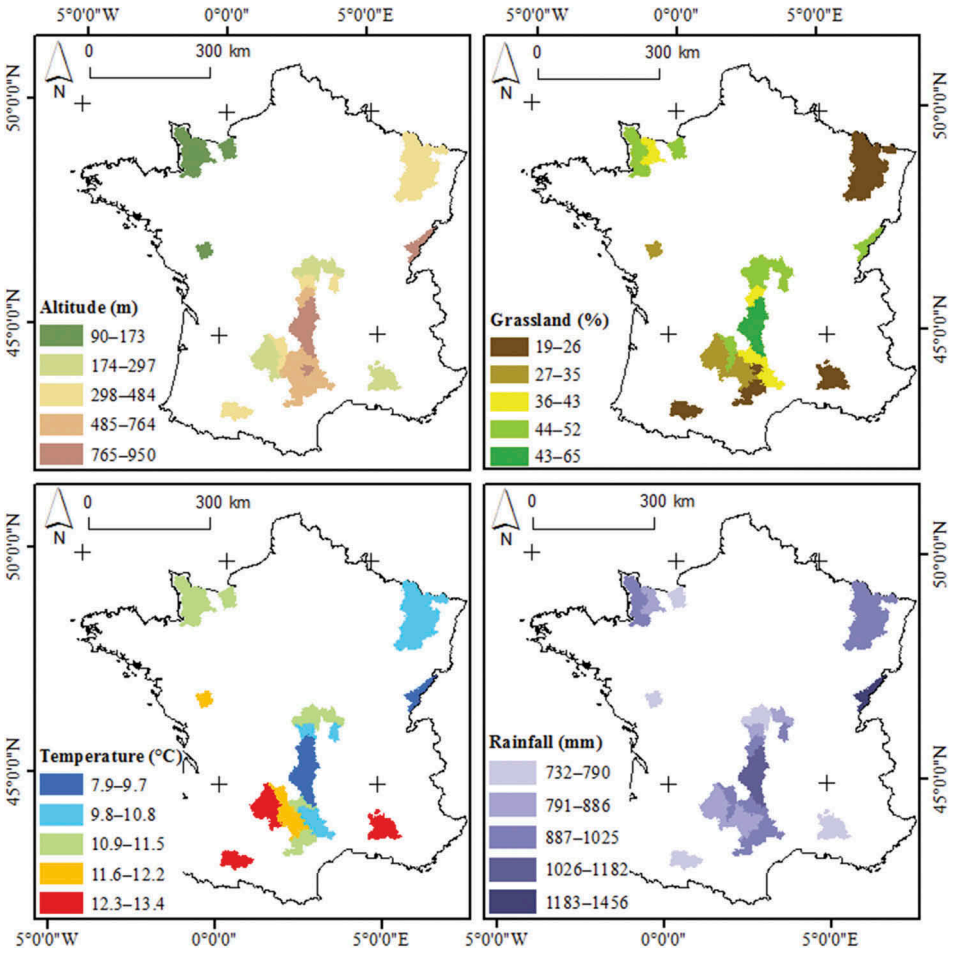

Figure 2. Characterization of the 25 FRs selected for the study according to altitude, grassland surface percentage, temperature, and rainfall, both averaged over 2003–2012.

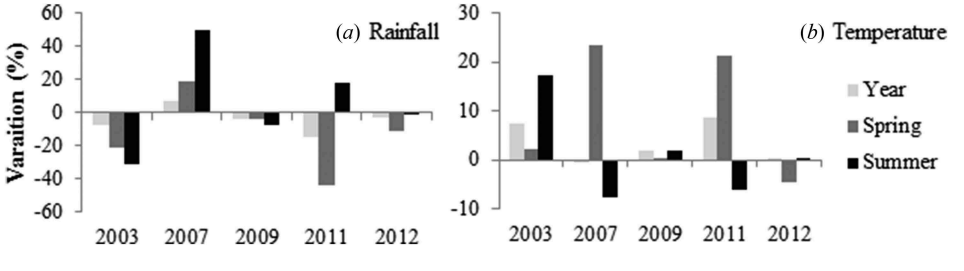

Figure 3. Annual, spring and summer (*a*) rainfall and (*b*) temperature variations for the five selected years compared to a historical reference (2003/2012) observed in the 25 FRs.

3.2. *Remote-sensing data*

In this study, biophysical products (*f*APAR and *f*Cover) are obtained from a biophysical inversion of daily reflectances image provided by Moderate Resolution Imaging Spectroradiometer (MODIS) and Medium Resolution Imaging Spectrometer (MERIS) sensors as described in Roumiguié, Jacquin, Sigel, Poilve, Lepoivre, et al. (2015). Products of the processing chain are 10 day synthesis of biophysical parameters delivered at 300 m spatial resolution. NDVI data come from the MODIS vegetation index product (MOD13Q1), distributed by the National Aeronautics and Space Administration (NASA) and the United States Geological Survey (USGS) and corresponding to 16 day synthesis at 250 m spatial resolution. NDVI is computed from atmospherically-corrected bi-directional surface reflectances that have been masked for water, clouds, heavy aerosols, and cloud shadows (Huete, Justice, and Van Leeuwen 1999).

Given the medium spatial resolution of the images, pixel reflectances may be composed of spectral responses from different land-cover types. A disaggregation method based on a statistical approach applied to reflectances is used to determine *f*APAR, *f*Cover, and NDVI for grassland (Faivre and Fischer 1997). This method estimates vegetation indices or biophysical parameters values for each land-cover class present in the mixed observation (determined from a land-cover map) and the *a priori* knowledge of each land-cover class's contribution to each pixel (local aspect) (Roumiguié, Jacquin, Sigel, Poilve, Lepoivre, et al. 2015). Consequently, *f*APAR, *f*Cover, and NDVI, relating to grassland cover, are calculated at an Elementary Statistical Unit (ESU) scale of 6 km×6 km.

Finally, the remote-sensing indices are averaged at the FR scale according to grassland surface in each ESU. Figure 4 illustrates the three time series of 'grassland' remote-sensing indices available for a FR in southern France in 2003.

3.3. *Climatic data*

Climatic data are provided by Météo-France. Visible radiation, rainfall, and temperature variables from the SAFRAN/F database (Quintana-Seguí, Le Moigne et al. 2008; Vidal, Martin et al. 2010) are selected. These reanalysis data are derived from a numerical weather model that incorporates station observations. These data are interpolated at an

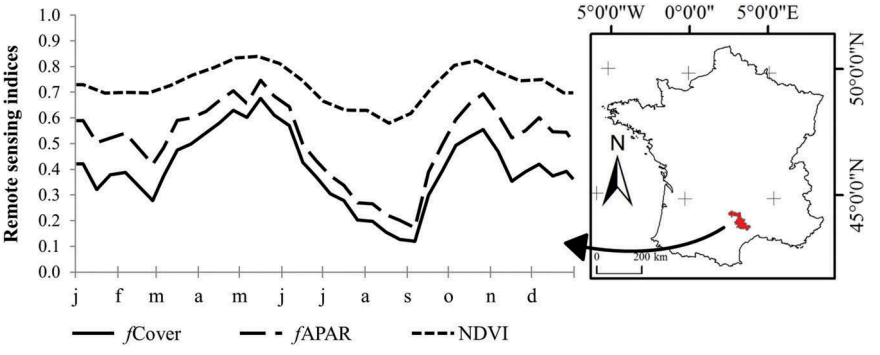

Figure 4. Example of the three time series of 'grassland' remote sensing indices available for a forage region situated in South of France in 2003.

8 km × 8 km grid using a digital elevation model and are available at a daily step. Time series of these variables are produced for each FR by averaging grid values within the area of interest. Additional climatic variables are calculated in order to introduce them in the computation of the different physiological effects modelled (see Section 2). The daily mean temperature (°C) is given by Equation (11):

$$t_i = \begin{cases} 18, if \frac{T_{\max,i}+T_{\min,i}}{2} > 18 \\ 0, if \frac{T_{\max,i}+T_{\min,i}}{2} < 0 \\ \frac{T_{\max,i}+T_{\min,i}}{2} \text{ otherwise} \end{cases}, \tag{11}$$

where $T_{\max,i}$ is the daily maximum air temperature and $T_{\min,i}$ is the daily minimum temperature.

Growing degree days correspond to the accumulated mean temperature (t_i) throughout the growing season (Equation (12)). Grassland phenology is driven by thermal time,

$$d_i = \sum_{i=(\mathrm{SOS})}^{I} t_i. \tag{12}$$

For the computation of the water stress index (W_i), the actual evapotranspiration (a_i) and the potential evapotranspiration (e_i) are, respectively, evaluated with daily rainfall (p_i) (Equation (13)) and the Jensen–Haise formula (Jensen and Haise 1963) (Equation (14)). Both are cumulated over the previous 30 days as recommended by Maselli, Argenti et al. (2013):

$$a_i = \sum_{i-30}^{I} p_i, \tag{13}$$

$$e_i = \sum_{i-30}^{I} \left(\frac{r_i}{L} \times 0.025 \times t_i + 0.08 \right), \tag{14}$$

where L is the latent heat of vaporization for water with a density of 1000 kg m^{-3} and at 20°C. (=2.45), r_i is the daily global radiation, and t_i is the daily mean temperature.

3.4 *Reference grassland production data*

Validation data are provided by the ISOP system (Donet, Ruget et al. 1999, 2000). In this system, grassland production estimated at a daily step for each FR with a mechanistic model adapted to grassland (Simulateur Multidisciplinaire pour les Cultures Standard – STICS Prairies) (Brisson, Mary et al. 1998), using climatic, soil, and grazing system data as inputs. Published data, delivered at FR scale, represent the variation of annual production compared to a historical reference (1982–2009). For the validation procedure, production data of the chosen FR/years are selected (Ruget F., personal communication). Figure 5 illustrates the spatial and temporal variations of production over the application sites (Ruget, Delécolle et al. 2001). It shows that two FRs have an average production higher than 8.1 tonnes of dry matter per hectare (t DM ha^{-1}) while three others are four times less (2.2 t DM ha^{-1}). Substantial variation around the average production exists

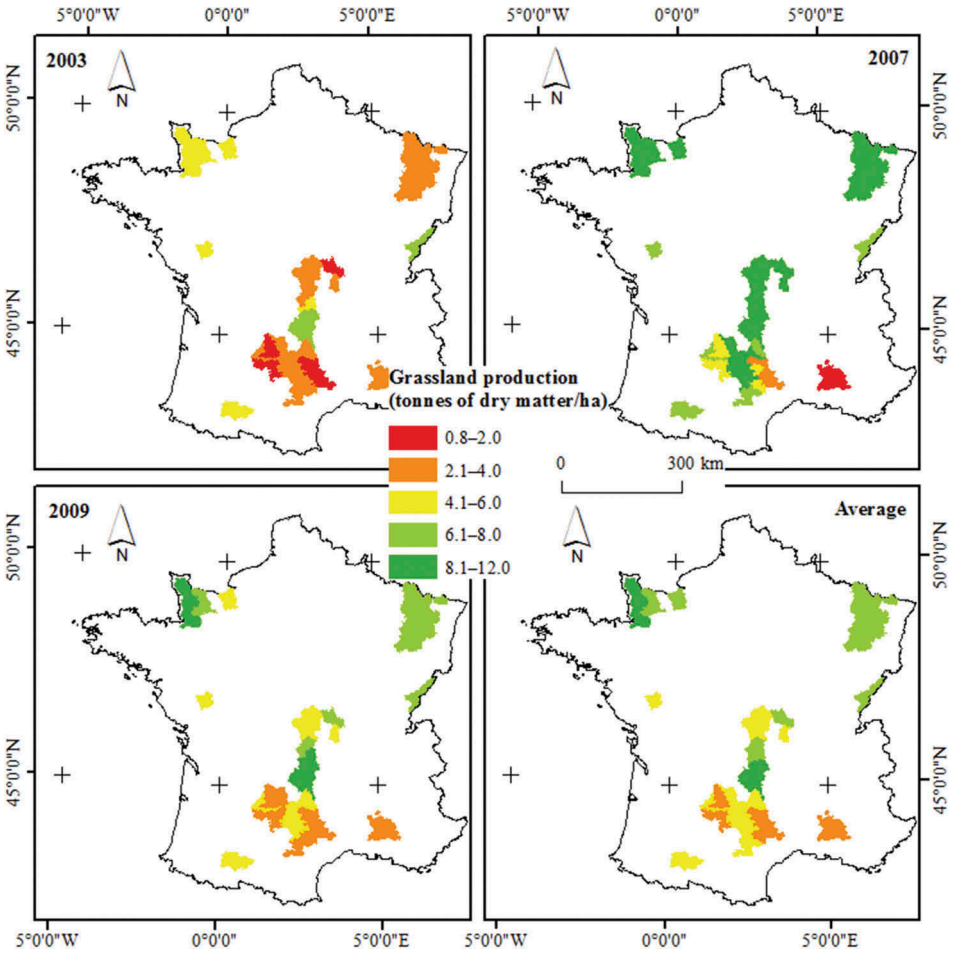

Figure 5. Grassland production, given by the ISOP model, of the 25 FRs selected for 2003, 2007, 2009 and in average of the 5 years studied.

due to inter-annual weather variability. For example, production during a dry year (2003) was substantially lower than during a humid year (2007).

3.5. *Methods*

3.5.1. *Model accuracy assessment*

A total of 768 models are tested against grassland production data. The models are the result of different combinations of factors (5) and various options to estimate each of them. These include three modalities for fraction of absorbed photosynthetically active radiation (factor 1); for RUE (factor 2), two modalities for temperature (T_i), season (S_i), phenology (G_i), and water stress (W_i); two modalities for PAR (factor 3); two modalities for leaf senescence modelling (D_i) (factor 4); for the growing season characteristics (factor 5), two modalities for the monitoring period (SOS/EOS) and the number of phenological cycles (m). The annual biomass production (B_n) obtained with these

models are evaluated by comparing each of them to grassland production estimates provided by the Information et Suivi Objectif des Prairies (ISOP) system (Y_n), considered to be the reference. We establish linear and power function regressions according to Equation (15).

Values for the power function are obtained to satisfy the assumption of a normal distribution of the residuals. To this end, a transformation of the dependent variable ($B_{n,z}$) is realized (Box and Cox 1964):

$$(Y_{n,z})^x = a \times B_{n,z} + b + \varepsilon, \tag{15}$$

where $Y_{n,z}$ is the validation production data, $B_{n,z}$ is the modelled production data for the year n and the forage region z, ε is the remaining error, a and b are parameters of the regression. For a linear regression function, x is equal to 1. For a power regression function, x is different to 1.

A k-fold cross validation is performed to determine the prediction error (Rodriguez, Perez, and Lozano 2010). For each model, the validation production dataset (containing 125 observations) is divided in threefold with 100 replications. Regression is trained on twofold (84 observations) and a measure of the performance is assessed with the remaining fold (42 observations). As the key performance criterion, we use the standardized root mean square error (SRMSE) given by the Equation (16), as it is a good indicator of a model predictive power (Loehlin 2004):

$$\mathrm{SRMSE} = \frac{\sqrt{\frac{\sum_{i=1}^{n} (Y_i - B_i)^2}{n}}}{\mathrm{SD}(Y_i)}, \tag{16}$$

where Y_i are the observed values, B_i are the modelled values, n is the number of observations and SD is the standard deviation.

Statistical tests on residuals are carried out to evaluate regression model validity. Residual normality and homoscedasticity are, respectively, assessed with Jarque–Bera (Jarque and Bera 1980)/Shapiro–Wilk (Royston 1992), and Breusch–Pagan (Breusch and Pagan 1979; Cook and Weisberg 1983) tests. All regressions with at least one of the statistical tests presenting a p-value less than 0.1 are excluded in order to select those that are the most robust and valid.

3.5.2. *Model inter-comparison procedure*

Figure 6 summarizes the comparison procedure between the baseline and new models. The first step consists of establishing regression models with linear and power functions using all the validation production data, resulting in an SRMSE and p-value for all models. The SRMSE provided by the baseline model is defined as a threshold ($\mathrm{SRMSE}_{\mathrm{Baseline}}$). Among the new models, only those that had valid statistical tests on residuals and an SRMSE value smaller than $\mathrm{SRMSE}_{\mathrm{Baseline}}$ are retained. For these models, analysis of the linear and power regression proportion enables identification of the best regression function type. Next, for each model, the value (x) that minimizes the SRMSE is selected by interpretation of the value (x) variation according to SRMSE.

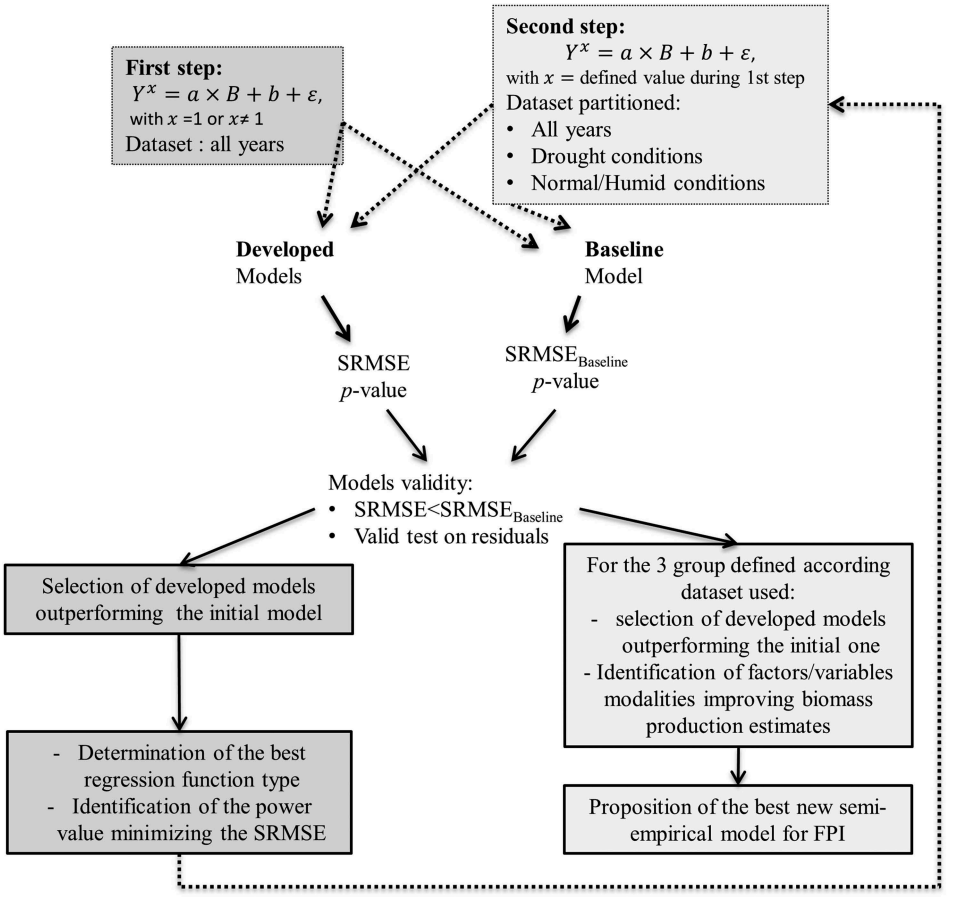

Figure 6. Overall procedural flowchart for inter-comparison of models.

In a second step, the validation production dataset is divided in two according to the climatic years. The objective is to examine the ability of the selected to accurately perform under different meteorological conditions. One set of data is composed of years 2003 and 2011, representing drought conditions resulting in low levels of biomass production. The other set contains 2007, 2009, and 2012 years and corresponds to humid or normal conditions with normal or above average biomass production. For the two sets, the same accuracy assessment is applied as for the full dataset.

Overall, three groups of models that outperformed the baseline model are obtained depending on whether the whole validation dataset is considered (group 1) or different validation datasets for dry years (group 2) and for humid or normal years (group 3). For each group, the factors/variable modalities that have been added in the developed models are observed to see how much they contribute in the improvement of the biomass production estimates.

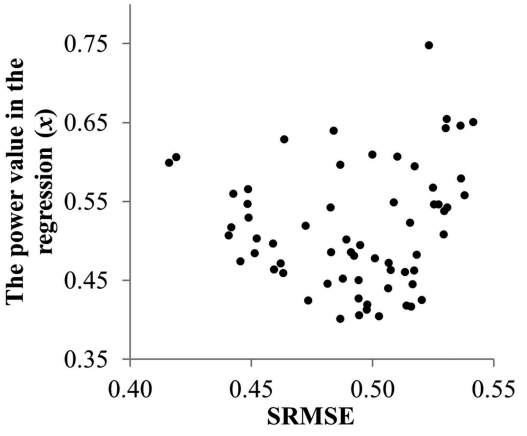

Figure 7. Scatterplots of the power value in the regression (x) and the SRMSE for the 64 models outperforming the baseline model.

4. Results

4.1. *Models overall performance estimation*

Given all possible combinations of the five factors added in the developed models, 768 models are tested. In relation to the complete validation dataset, model inter-comparison indicates that 64 developed models outperform the baseline model based on the SRMSE. Of these models, for 91% (including the baseline model) the SRMSE is smaller when applying a power function. Consequently, the power function, rather than a linear function is retained for consecutive analysis.

Figure 7 presents the scatterplot of the power value (x) and the SRMSE of the 64 models outperforming the baseline model. Smallest SRMSE values tend to be obtained with values for x of approximately 0.5–0.6. This suggests a quadratic link between observed and modelled biomass production data, illustrated for the baseline model in Figure 8. With a linear function, $SRMSE_{Baseline}$ is equal to 0.57 and coefficient of determination (R^2) to 0.68 (Figure 8(*a*)) whereas with a power function, $SRMSE_{Baseline}$ is equal to 0.54 and R^2 to 0.71 (Figure 8(*b*)). We decide to fix the power value (x) for all models to 0.50 in order to have a more consistent comparison between models and reduce overfitting problems. When reconsidering all 768 models and fixing x to 0.5, a total of 74 models outperform the baseline model. The best model is based on a biomass production function using the *f*Cover accumulated over a variable monitoring period and integrating the water stress and season effects. For this model, the SRMSE is 0.42 and the R^2 = 0.83 (Figure 8(*c*)). Precision of biomass prediction is 23% higher than with the baseline model.

When dividing the validation dataset into dry and normal/humid years, the baseline model performs better in normal or humid conditions ($SRMSE_{Baseline}$ = 0.63 for dry; $SRMSE_{Baseline}$ = 0.52 for normal/humid). For this division, fewer models improve the production estimates in normal or humid conditions (38 of 74 with an average improvement of 7% and a maximum of 20%) than for the dry condition (67 of 74 with an

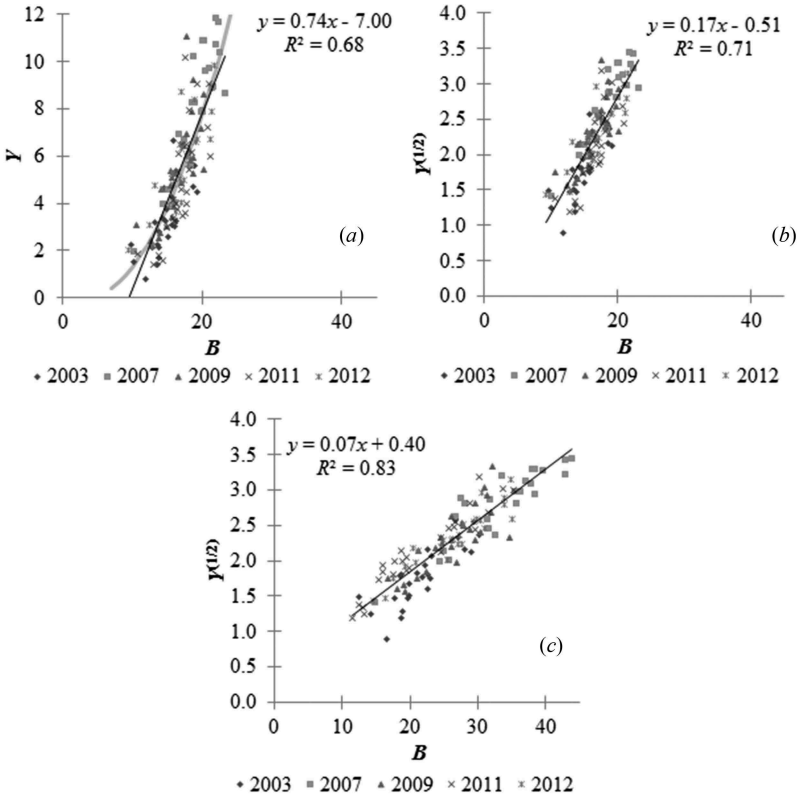

Figure 8. Scatterplots of the baseline model with (*a*) linear and (*b*) power regression functions ($x = 0.50$) between the observed (Y) and modelled (B) productions with the baseline model and considering the whole validation dataset. Dashed black line highlights the power function link between the two datasets. (c) Scatterplots of the power regression function ($x = 0.50$) between the observed (Y) and modelled (B) productions with the best performing model.

average improvement of 9% and a maximum of 22%) as compared to the baseline model. Figure 9 presents the scatterplots between the observed (*Y*) and modelled (*B*) productions for the (*a*) baseline model and (*b*) best models estimated by considering only either dry years (2003 and 2011) or normal/humid years (2007, 2009, and 2012). The best model for dry years is more complex (incorporating *f*Cover cumulated over a variable monitoring period, water stress, season, temperature, and radiation) than for normal/humid years (*f*Cover accumulated over a variable monitoring period and water stress).

In conclusion, the baseline model performs well irrespective of the group of years considered. This confirms the earlier FPI validation results obtained in previous studies (Roumiguié, Jacquin, Sigel, Poilve, Hagolle, et al. 2015, Roumiguié, Jacquin, Sigel, Poilve, Lepoivre, et al. 2015) and corroborates findings of Jung, Verstraete et al. (2008) that recommended using an empirical model based on a remote-sensing index to estimate biomass production. But, results of the performance analysis lead to the identification of two sources of improvements for the FPI computation method:

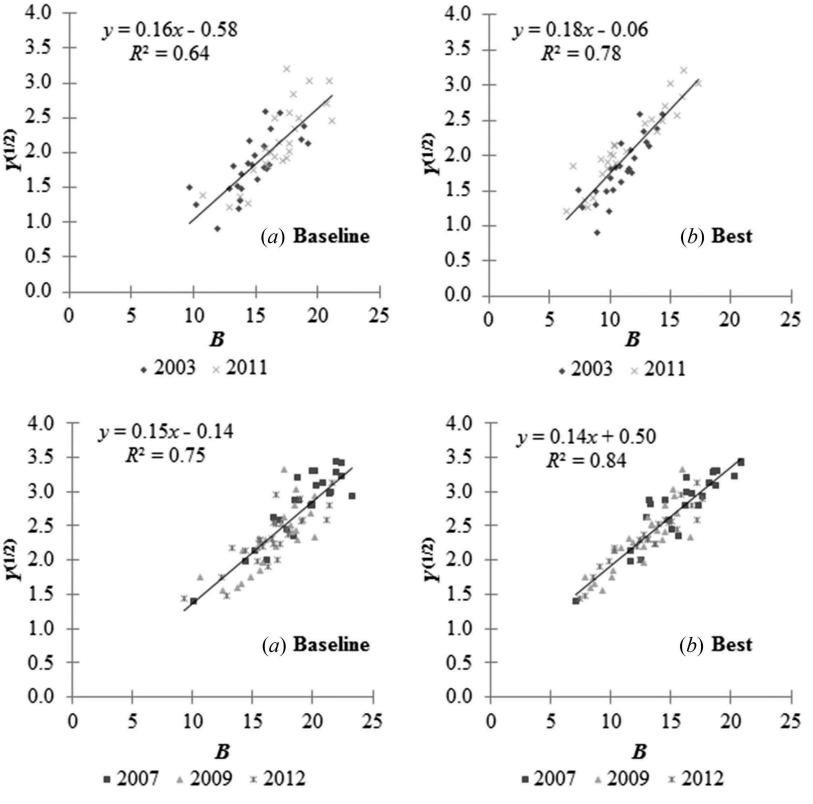

Figure 9. Scatterplots between the observed (Y) and modelled (B) productions of the (*a*) baseline and (*b*) best developed model estimated by considering only either drought years (2003 and 2011) or normal/humid years (2007, 2009, and 2012).

(1) use of a power function instead of a linear function;
(2) integrating ancillary data in semi-empirical models corroborating the conclusions of Seaquist, Olsson, and Ardö (2003).

4.2. *Individual assessment of biomass production function factors*

For the 74 models that outperform the baseline model and classified according to the climatic context (group 1: all years; group 2: dry years; group 3: normal/humid years), the distribution of variables/factors tested is analysed. Results are presented in Table 2. Models based on a biophysical parameter (*f*APAR, *f*Cover) perform in general better than models based on NDVI (89% or more of the developed models are based on a biophysical parameter), with a preference for *f*Cover. Further, inclusion of the water stress effect results in a significant improvement for FPI computation, especially during drought. We find that the RUE should be estimated at least with the water stress effect but not with the senescence function (92–96% of developed models do not contain the senescence function). The fraction of models that used temperature, phenology and season effects are about 50%, suggesting the need for further analysis of its importance. PAR is not found to be an important element for the models. Finally, looking for a unique FPI

Table 2. Distribution in percentage of the variable/factor tested with the different validation dataset.

Variables/factors	Group 1 (n = 74)	Group 2 (n = 67)	Group 3 (n = 38)
*f*Cover/*f*APAR/NDVI	**61**/31/8	**63**/34/3	**68**/21/11
PAR, no/yes	**61**/39	**57**/43	**92**/8
Temperature, no/yes	**55**/45	**54**/46	**68**/32
Phenology, no/yes	47/**53**	48/**52**	45/**55**
Water stress, no/yes	14/**86**	12/**88**	16/**84**
Season, no/yes	49/**51**	**51**/49	50/50
Senescence, no/yes	**96**/4	**96**/4	**92**/8
Monitoring period Fixed/variable	30/**70**	31/**69**	21/**79**
Phenological cycle, 1/2	**67**/33	**63**/37	**76**/24

n indicates the number of models in each group. Numbers in bold correspond to the majority.

model for all grassland in France, the growing season has to be modelled as uni-modal growth cycle and with a monitoring period variable in space and time.

Based on these results, a new semi-empirical model for the FPI can be defined with the Equation (17) to compute the annual biomass production and improve the baseline model given by Equation (1):

$$B_n = \sum_{i=(\mathrm{SOS})}^{(\mathrm{EOS})} (f\mathrm{Cover\ Grassland})_i \times (\mathrm{RUE})_i, \tag{17}$$

where the RUE_i is equal to the W_i (see Equation (8)) and SOS/EOS values are determined annually at the FR scale from the analysis of the *f*Cover time series.

Among the 34 developed models outperforming the baseline model across all validation datasets, eight correspond to Equation (17) with an average improvement with baseline's SRMSE of 18.6%. Table 3 shows the contributions of the SOS/EOS and RUE factors, independently or combined, to the improvement of estimate precision through the SRMSE. Distribution of the residuals for the baseline and best developed models are given in Figure 10. Both factors are relevant to improve the precision of biomass estimates given by the baseline model. But, with a decrease of the baseline SRMSE and an increase of the baseline R^2 of −13% and +10%, respectively, the RUE factor estimated with the water stress effect seems to contribute more than the SOS/EOS factor. This result confirms the important role of the RUE factor and the water stress index to better estimate grassland biomass production. Results of statistical tests (normality and homoscedasticity) are also provided in Table 3 to complete models performance analysis. Compared to the baseline model, the significance of the variables is confirmed with a more stable model.

5. Discussion

The basic idea assessed here is that production efficiency model (PEM) principle integrating meteorological data should improve the baseline FPI model. Opposed to this idea is the advice expressed among others by Coops, Ferster et al. (2009) to run models with less demanding data rather than considering that exogenous variables are correctly mapped and improve estimates. In this section, we discuss:

Table 3. Contribution of SOS/EOS and RUE factors to the improvement of the precise estimation of biomass production.

Model	Equation	SRMSE	R^2	*p*-Value for statistical tests		
				Breusch–Pagan	Jarque–Bera	Shapiro–Wilk
Baseline model	$Y_{n,z} = 0.74 \times B_{n,z} - 7.00 + \varepsilon$	0.57	0.68	**0.09**	0.02	0.02
Baseline model	$(Y_{n,z})^{0.5} = 0.17 \times B_{n,z} - 0.51 + \varepsilon$	0.54	0.71	**0.76**	**0.49**	**0.39**
Baseline model with SOS/EOS only	$(Y_{n,z})^{0.5} = 0.15 \times B_{n,z} + 0.12 + \varepsilon$	0.49 (−9%)	0.76 (+7%)	**0.94**	**0.50**	**0.78**
Baseline model with RUE only	$(Y_{n,z})^{0.5} = 0.16 \times B_{n,z} + 0.03 + \varepsilon$	0.47 (−13%)	0.78 (+10%)	**0.51**	**0.13**	**0.21**
Best developed model with SOS/EOS and RUE	$(Y_{n,z})^{0.5} = 0.07 \times B_{n,z} + 0.40 + \varepsilon$	0.42 (−22%)	0.83 (+17%)	**0.85**	**0.71**	**0.90**

Statistical interpretation: numbers in bold indicate *p*-value > α with $\alpha = 0.05$ meaning null hypothesis (either homoscedasticity or normality of residuals) cannot be rejected.

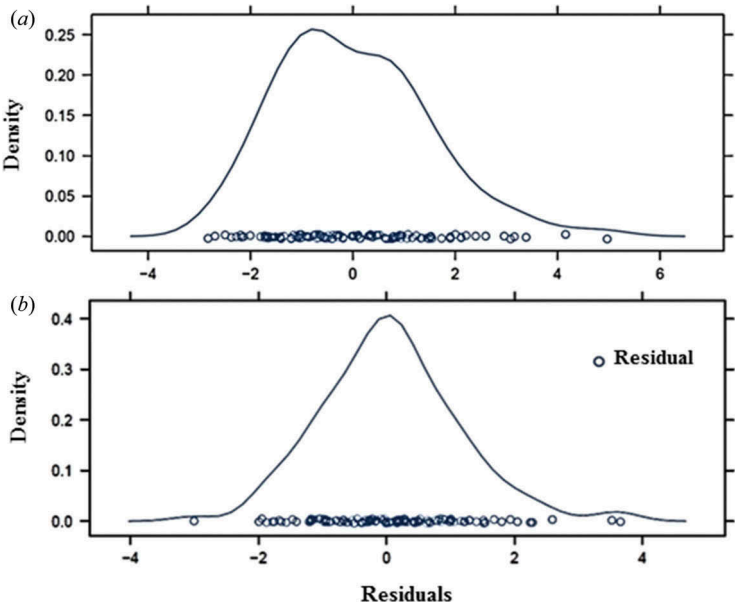

Figure 10. Distribution of the residuals for the (*a*) baseline and (*b*) best developed models.

(1) which variables/factors improve estimates and how they should be integrated in an operational context;
(2) which variables/factors are not relevant and should be abandoned or studied further;
(3) how satellite images provided by new sensors and evolution of methodology in PEM could reduce basis risk in index-based insurance.

5.1. *On the operational implementation of identified improving factors*

Two tested factors are clearly identified as key improvements in the FPI computation: incorporating the RUE including the water stress RUE reduction, and accounting for spatial and temporal variability of the growing season. The RUE as moderated by the water stress index (Maselli, Argenti et al. 2013) proved effective for the generation of more accurate FPI models. Nonetheless, its inclusion would require an operational (near real time) access to accurate meteorological variables (temperature, rainfall, and radiation) (de Leeuw, Vrieling et al. 2014).

The second major improvement concerns the implementation of a variable monitoring period. Meroni, Verstraete et al. (2014) showed that a properly identified start and end of season contributes to a better production estimate. In fact, forage insurance programmes in East Africa also incorporate a spatially variable period for integrating NDVI, based on phenological analysis of NDVI time series (Vrieling, Meroni et al. 2016). A limitation of our study is the developed methodology to observe phenological indicators. For this study we applied an empirical (visual) analysis of the remote-sensing index temporal profiles and did not implement an automated approach. We acknowledge that this should be in principle easy to achieve in future, given that a good range of methods

has been developed for the extraction of phenological parameters from image time series (Beurs and Henebry 2010; Meroni, Verstraete et al. 2014).

5.2. *Explanations for why potential improving factors are not relevant*

Results obtained for the temperature effect and radiation are not in agreement with literature. For the first one, our hypothesis is that the size of the geographic unit used to establish the regression between observed and modelled annual grassland production is too coarse and as a consequence results in smooth RUE values. This makes that extreme local temperatures are not well represented at the FR scale, because they are averaged over a large area (median equals 184,933 ha for the 25 FR). At the municipality level (approximately 1500 ha) corresponding to FPI scale computation, we expect that temperature extremes may be better represented and consequently its effect on photosynthesis may be more realistic (Cai, Yuan et al. 2014). So, it may still be relevant to incorporate the temperature effect in the RUE computation when focussing on smaller areas.

Our results suggest that PAR does not need to be integrated into the new model, as also recommended by Piñeiro, Oesterheld, and Paruelo (2006). While on the one hand this may cause an incomplete representation of the PEM, other studies also reveal a negative correlation between gross primary production (GPP) and global radiation (PAR) in grassland over the globe (Beer, Reichstein et al. 2010; Cai, Yuan et al. 2014) with high levels of insolation leading to high photosynthetic rate but also to high temperatures and evapotranspiration rates, thereby increasing the water stress. In addition, as Quintana-Seguí, Le Moigne et al. (2008) explain in their study, radiation provided by the SAFRAN/F Database present an important RMSE, which could lead to decrease new model accuracy instead of increasing it.

The phenology effect (G_i), the senescence leaf modelling (D_i) and the possibility of having a variable number of phenological cycles while modelling the growing season (m), do not contribute to better models in our framework. This result is in contradiction with literature (Cros, Duru et al. 2003; Duru, Adam et al. 2009; Vrieling, Meroni et al. 2016). For the phenology effect (G_i) and the senescence leaf modelling (D_i), they are traditionally parameterized at species level or using plant functional traits characteristics (Duru, Adam et al. 2009). It requires *a priori* knowledge on the detailed grassland species composition. In our study, given the spatial resolution of remote-sensing images (300 m) used to characterize grassland vegetation condition, it is not possible to work at this particular level. So, we consider grasslands as mono-species where phenological developments are not species-dependent and use a common parameterization for all grassland types. For the number of phenological cycles while modelling the growing season (m), Vrieling, Meroni et al. (2016) find it relevant because of the existence of two important growth grassland cycles within the year as observed in Kenya. In the case of France, the usefulness of this variable does not seem to be so important. Annual grassland production is mainly driven by the spring period (around 75%) (Pottier, Michaud et al. 2012). For all these reasons, these three factors should not be further considered as potential improvements. On this account, we, therefore, support McCallum, Wagner et al. (2009) suggesting that the FPI model has to keep a reasonably low level of complexity in order to be practical and operational.

5.3. *On the potential of additional remote-sensing data to bring improvements*

First, it is of interest to consider other variables in the FPI computation to estimate RUE factor. The water stress index (W_i) and the temperature effect (T_i) are obtained from three climatic variables (temperature, rainfall, and radiation) provided by SAFRAN-Meteo-France. This database is only available for research purposes and cannot be used by private companies for commercial purposes. In the framework of the development of a commercial product, it is mandatory to identify other reliable data sources that can be used in future and are available in near real time. Beyond existing weather station networks and databases collecting *in situ* measurements, climatic variables estimated from remotely sensed data constitutes an exploratory field in both PEMs and index-based Insurance. For example, NASA provides evapotranspiration data (MOD16) with a spatial resolution of 1 km and a temporal resolution of 8 days. These data are employed for global modelling of GPP (Yang, Guan et al. 2014). Rainfall estimates are also available from thermal infrared and passive micro-wave sensors (Dinku, Funk, and Grimes 2008; Hellmuth, Osgood et al. 2009). Such operational data sources should be further tested within our model comparison framework.

Second, higher spatial and temporal resolution remote-sensing data provided by the new generation of sensors such as Sentinel-2 have the potential of improving the accuracy of PEMs for grassland productivity estimation. Direct monitoring of grassland vegetation activity at the scale of the plot becomes possible. There are three main consequences:

(1) the error in the production estimation attached to the disaggregation step, compulsory while processing moderate spatial resolution remote-sensing data could reduce (Roumiguié, Jacquin, Sigel, Poilve, Lepoivre, et al. 2015), which in turn can decrease the basis risk;
(2) factors and parameters relying on plant functional traits can be considered in the modelling stage as, at the plot scale, grassland species differentiation is possible;
(3) the potential of application of the FPI is increased with new opportunities to use it in countries where ground reference data to run calibration/validation of the model at the required spatial scale are lacking (Rembold, Atzberger et al. 2013).

6. Conclusion

To improve an index-based insurance product for grassland production in France, 768 models are tested to estimate biomass production based on all possible combinations of five factors studied. Outputs are compared with data provided by a mechanistic model (ISOP system) over a sample of 25 forage regions and for 5 contrasted climatic years (humid, normal and dry). Our results reveal that:

(1) the baseline model based on the *f*Cover integral gives satisfactory results (SRMSE = 0.57 and R^2 = 0.68);
(2) a quadratic link characterizes the relationship between the observed and estimated biomass production values and a power regression function (x = 0.5) is proposed to increase quality and robustness of our estimates (SRMSE = 0.54 and R^2 = 0.71);

(3) among the developed models, 34 outperform the baseline regardless of the climatic context and lead to increased accuracy of production estimates;
(4) from these findings, a new semi-empirical model for FPI is defined to compute the annual biomass production and improve the baseline model (SRMSE = 0.42 and R^2 = 0.83). It is still based on *f*Cover but enriched with a water stress index and the phenological indicators SOS/EOS that are spatially and temporally variable according to the grassland growth cycle given by the *f*Cover temporal profile. From the best 34 models identified, 8 correspond to this new FPI model and provide, on average, a decrease of the SRMSE of 18.6 % compared to the $SRMSE_{Baseline}$.
(5) While the results obtained with many of the factors included in the new FPI model corroborate findings in the literature, results for others tested factors are not in agreement with previous studies as they do not increase the models' quality (McCallum, Wagner et al. 2009; Cai, Yuan et al. 2014). We conclude that, phenological and season effects in the RUE factor, the PAR factor, the senescence leaf modelling, and consideration of multiple phenological cycles (*m*) for grasslands within a year should not be included in the new FPI model. However, concerning the temperature effect on photosynthesis and its relevance highlighted in the literature (Duru, Adam et al. 2009), further investigation is warranted using validation data at finer spatial scales.

Acknowledgements

The authors thank Françoise Ruget of French National Institute of Agronomy for providing the grassland production estimates from the ISOP system in order to achieve the validation exercise, Bruno Lepoivre and Crédit Agricole Pacifica Assurances for their support, and Shawn Hutchinson of Geography Department of Kansas State University for his help in reviewing English language of this article.

Disclosure statement

No potential conflict of interest was reported by the authors.

References

Agriculture Financial Services Corporation. 2014. Protection for Perennial Crops, AFSC: 88.
Agroasemex. 2006. *La experiencia mexicana en el desarollo y operacion de seguros paramétricos orientados a la ganaderia*. Santiago de Queretaro: Agroasemex.
Agroseguro. 2012. *Consulta de indices de vegetacion para seguros por teledeteccion. Informe annual*. Madrid: Agroseguro.
Asner, G. P., C. A. Wessman, and S. Archer. 1998. "Scale Dependence of Absorption of Photosynthetically Active Radiation in Terrestrial Ecosystems." *Ecological Applications* 8 (4): 1003–1021. doi:10.1890/1051-0761(1998)008[1003:SDOAOP]2.0.CO;2.
Baret, F., M. Weiss, D. Allard, M. Leroy, H. Jeanjean, R. Fernandes, R. Myneni, J. Privette, and J. Morisette. 2005. "VALERI: A Network of Sites and a Methodology for the Validation of Medium Spatial Resolution Land Satellite Products." *Remote Sensing of Environment*.

Barnett, B. J., and O. Mahul. 2007. "Weather Index Insurance for Agriculture and Rural Areas in Lower-Income Countries." *American Journal of Agricultural Economics* 89 (5): 1241–1247. doi:10.1111/ajae.2008.89.issue-5.

Beer, C., M. Reichstein, E. Tomelleri, P. Ciais, M. Jung, N. Carvalhais, C. Rödenbeck, M. A. Arain, D. Baldocchi, and G. B. Bonan. 2010. "Terrestrial Gross Carbon Dioxide Uptake: Global Distribution and Covariation with Climate." *Science* 329 (5993): 834–838. doi:10.1126/science.1184984.

Bergeot, S. 2015. "PacAn Analysis of Transformationsifica lance l'assurance des prairies pour 2016." *La France Agricole* 3592: 14.

Beurs, K., and G. Henebry. 2010. "Spatio-Temporal Statistical Methods for Modelling Land Surface Phenology." In *Phenological Research*, edited by I. L. Hudson and M. R. Keatley, 177–208. Netherlands: Springer.

Box, G. E., and D. R. Cox. 1964. "An Analysis of Transformations." *Journal of the Royal Statistical Society. Series B (Methodological)* 26 (2): 211–252.

Boyer, P. 2008. "Assurer les calamités agricoles?" *Notes et études économiques du Ministère de l'Agriculture* 30: 7–32.

Breusch, T. S., and A. R. Pagan. 1979. "A Simple Test for Heteroscedasticity and Random Coefficient Variation." *Econometrica: Journal of the Econometric Society* 47: 1287–1294. doi:10.2307/1911963.

Brisson, N., B. Mary, D. Ripoche, M. H. Jeuffroy, F. Ruget, B. Nicoullaud, P. Gate, F. Devienne-Barret, R. Antonioletti, and C. Durr. 1998. ""STICS: A Generic Model for the Simulation of Crops and Their Water and Nitrogen Balances. I. Theory and Parameterization Applied to Wheat and Corn." *Agronomie* 18 (5–6): 311–346. doi:10.1051/agro:19980501.

Cai, W., W. Yuan, S. Liang, S. Liu, W. Dong, Y. Chen, D. Liu, and H. Zhang. 2014. "Large Differences in Terrestrial Vegetation Production Derived from Satellite-Based Light Use Efficiency Models." *Remote Sensing* 6 (9): 8945–8965. doi:10.3390/rs6098945.

Camacho, F., and J. Cernicharo. 2011. ""Geoland2. Validation Report Medium Resolution (MERIS) Vegetation Parameters." Geoland2, EOLAB. 62.

Camacho, F., and I. Torralba. 2010. "Geoland2. Validation Report High Resolution Vegetation Parameters." Geoland2, EOLAB. 65.

Ceccato, P., M. Brown, C. Funk, C. Small, E. Holthaus, A. Siebert, and N. Ward. 2008. "Remote Sensing Vegetation." In *Index Insurance and Climate Risk: Prospects for Development and Disaster Management*, edited by M. E. Hellmuth, D. E. Osgood, U. Hess, A. Moorhead, and H. Bhojwani. New York: Columbia University.

Cook, R. D., and S. Weisberg. 1983. "Diagnostics for Heteroscedasticity in Regression." *Biometrika* 70 (1): 1–10. doi:10.1093/biomet/70.1.1.

Coops, N. C., C. J. Ferster, R. H. Waring, and J. Nightingale. 2009. "Comparison of Three Models for Predicting Gross Primary Production across and within Forested Ecoregions in the Contiguous United States." *Remote Sensing of Environment* 113 (3): 680–690.

Courault, D., R. Hadria, F. Ruget, A. Olioso, B. Duchemin, O. Hagolle, and G. Dedieu. 2010. "Combined Use of FORMOSAT-2 Images with a Crop Model for Biomass and Water Monitoring of Permanent Grassland in Mediterranean Region." *Hydrology and Earth System Sciences* 14 (9): 1731–1744. doi:10.5194/hess-14-1731-2010.

Crédit Agricole. 2013. "Satellite et assurance, un couple en orbite." *Crédit Agricole Magazine* 119: 18–19.

Cros, M. J., M. Duru, F. Garcia, and R. Martin-Clouaire. 2003. "A Biophysical Dairy Farm Model to Evaluate Rotational Grazing Management Strategies." *Agronomie* 23 (2): 105–122. doi:10.1051/agro:2002071.

de Leeuw, J., A. Vrieling, A. Shee, C. Atzberger, K. Hadgu, C. Biradar, H. Keah, and C. Turvey. 2014. "The Potential and Uptake of Remote Sensing in Insurance: A Review." *Remote Sensing* 6 (11): 10888–10912. doi:10.3390/rs61110888.

Delécolle, R., S. J. Maas, M. Guérif, and F. Baret. 1992. "Remote Sensing and Crop Production Models: Present Trends." *ISPRS Journal of Photogrammetry and Remote Sensing* 47 (2–3): 145–161. doi:10.1016/0924-2716(92)90030-D.

Di Bella, C., R. Faivre, F. Ruget, B. Seguin, M. Guerif, B. Combal, A. Weiss, and C. Rebella. 2004. "Remote Sensing Capabilities to Estimate Pasture Production in France." *International Journal of Remote Sensing* 25 (23): 5359–5372. doi:10.1080/01431160410001719849.

Dinku, T., C. Funk, and D. Grimes. 2008. "The Potential of Satellite Rainfall Estimates for Index Insurance." In *Index Insurance and Climate Risk: Prospects for Development and Disaster Management*, edited by M. E. Hellmuth, D. E. Osgood, U. Hess, A. Moorhead, and H. Bhojwani. New York: Columbia University.

Donet, I., F. Ruget, C. Le Bas, and V. Rabaud. 2000. "Guide d'utilisation d'ISOP. Agreste, Chiffres et Données Agriculture." *Montreuil sous-bois* 134: 55.

Donet, I., F. Ruget, V. Rabaud, V. Pérarnaud, R. Delécolle, and N. Bonneviale. 1999. "ISOP: An Integrated System to Real-Time Assessment of Forage Production Variability over France." European Conference, Norrkoping, September 13–17, 4.

Duru, M., M. Adam, P. Cruz, G. Martin, P. Ansquer, C. Ducourtieux, C. Jouany, J. P. Theau, and J. Viegas. 2009. "Modelling Above-Ground Herbage Mass for a Wide Range of Grassland Community Types." *Ecological Modelling* 220 (2): 209–225. doi:10.1016/j.ecolmodel.2008.09.015.

Duru, M., P. Cruz, G. Martin, J. P. Theau, M. H. Charron, M. Desange, C. Jouany, and A. Zerourou. 2010. "Herb'sim, a Model for a Rational Management of Grass Production and Grass Utilization." *Fourrages* 210: 37–46.

Dusseux, P., L. Hubert-Moy, T. Corpetti, and F. Vertès. 2015. "Evaluation of SPOT Imagery for the Estimation of Grassland Biomass." *International Journal of Applied Earth Observation and Geoinformation* 38: 72–77. doi:10.1016/j.jag.2014.12.003.

Faivre, R., and A. Fischer. 1997. "Predicting Crop Reflectances Using Satellite Data Observing Mixed Pixels." *Journal of Agricultural, Biological, and Environmental Statistics* 2 (1): 87–107. doi:10.2307/1400642.

Field, C. B., J. T. Randerson, and C. M. Malmström. 1995. "Global Net Primary Production: Combining Ecology and Remote Sensing." *Remote Sensing of Environment* 51 (1): 74–88. doi:10.1016/0034-4257(94)00066-V.

Gaitán, J. J., D. Bran, G. Oliva, G. Ciari, V. Nakamatsu, J. Salomone, D. Ferrante, et al. 2013. "Evaluating the Performance of Multiple Remote Sensing Indices to Predict the Spatial Variability of Ecosystem Structure and Functioning in Patagonian Steppes." *Ecological Indicators* 34: 181–191. doi:10.1016/j.ecolind.2013.05.007.

Gao, T., B. Xu, X. Yang, Y. Jin, H. Ma, J. Li, and H. Yu. 2013. "Using MODIS Time Series Data to Estimate Aboveground Biomass and Its Spatio-Temporal Variation in Inner Mongolia's Grassland between 2001 and 2011." *International Journal of Remote Sensing* 34 (21): 7796–7810. doi:10.1080/01431161.2013.823000.

Geeraert, J.-M. 2012. *L'assurance récoltes : L'exemple de Pacifica*. Paris: Séances hebdomadaire de l'AAF.

Gilabert, M. A., A. Moreno, F. Maselli, B. Martínez, M. Chiesi, S. Sánchez-Ruiz, F. J. García-Haro, et al. 2015. "Daily GPP Estimates in Mediterranean Ecosystems by Combining Remote Sensing and Meteorological Data." *ISPRS Journal of Photogrammetry and Remote Sensing* 102: 184–197. doi:10.1016/j.isprsjprs.2015.01.017.

Gosse, G., C. Varlet-Grancher, R. Bonhomme, M. Chartier, J.-M. Allirand, and G. Lemaire. 1986. "Production maximale de matière sèche et rayonnement solaire intercepté par un couvert végétal." *Agronomie* 6 (1): 47–56. doi:10.1051/agro:19860103.

Hazell, P. R., and U. Hess. 2010. "Drought Insurance for Agricultural Development and Food Security in Dryland Areas." *Food Security* 2 (4): 395–405. doi:10.1007/s12571-010-0087-y.

Hellmuth, M. E., D. E. Osgood, U. Hess, A. Moorhead, and H. Bhojwani, eds. 2009. *Index Insurance and Climate Risk: Prospects for Development and Disaster Management*. New York, USA: Climate and Society. Columbia University, International Research Institute for Climate and Society (IRI).

Hentgen, A. 1982. "Une méthode pour améliorer la connaissance de la production disponible des surfaces herbagères au niveau national." *Fourrages* 92: 15–49.

Huete, A., K. Didan, T. Miura, E. P. Rodriguez, X. Gao, and L. G. Ferreira. 2002. "Overview of the Radiometric and Biophysical Performance of the MODIS Vegetation Indices." *Remote Sensing of Environment* 83 (1–2): 195–213. doi:10.1016/S0034-4257(02)00096-2.

Huete, A., C. Justice, and W. Van Leeuwen. 1999. *MODIS Vegetation Index (MOD13) Algorithm Theoretical Basis Document*. Greenbelt: NASA Goddard Space Flight Centre.

Jarque, C. M., and A. K. Bera. 1980. "Efficient Tests for Normality, Homoscedasticity and Serial Independence of Regression Residuals." *Economics Letters* 6 (3): 255–259. doi:10.1016/0165-1765(80)90024-5.

Jensen, M. E., and H. R. Haise. 1963. "Estimating Evapotranspiration from Solar Radiation." *Proceedings of the American Society of Civil Engineers, Journal of the Irrigation and Drainage Division* 89: 15–41.

Jin, Y., X. Yang, J. Qiu, J. Li, T. Gao, Q. Wu, F. Zhao, H. Ma, H. Yu, and B. Xu. 2014. "Remote Sensing-Based Biomass Estimation and Its Spatio-Temporal Variations in Temperate Grassland, Northern China." *Remote Sensing* 6 (2): 1496–1513. doi:10.3390/rs6021496.

Jouven, M., P. Carrère, and R. Baumont. 2006. "Model Predicting Dynamics of Biomass, Structure and Digestibility of Herbage in Managed Permanent Pastures. 1. Model Description." *Grass and Forage Science* 61 (2): 112–124. doi:10.1111/j.1365-2494.2006.00515.x.

Jung, M., M. Verstraete, N. Gobron, M. Reichstein, D. Papale, A. Bondeau, M. Robustelli, and B. Pinty. 2008. "Diagnostic Assessment of European Gross Primary Production." *Global Change Biology* 14 (10): 2349–2364. doi:10.1111/gcb.2008.14.issue-10.

Launay, M., and M. Guerif. 2005. "Assimilating Remote Sensing Data into a Crop Model to Improve Predictive Performance for Spatial Applications." *Agriculture, Ecosystems & Environment* 111 (1–4): 321–339. doi:10.1016/j.agee.2005.06.005.

Lemaire, G., D. Micol, L. Delaby, J. Fiorelli, M. Duru, and F. Ruget. 2006. ""ESCo - Sécheresse et agriculture" - Sensibilité à la sécheresse des systèmes fourragers et de l'élevage des herbivores Sécheresse et agriculture: réduire la vulnérabilité de l'agriculture à un risque accru de manque d'eau." Rapport de l'expertise scientifique collective réalisée par l'Inra à la demande du ministère de l'Agriculture et de la Pêche, INRA. Chapitre 1.1.4, 88–108.

Loehlin, J. C. 2004. *Latent Variable Models: An Introduction to Factor, Path, and Structural Equation Analysis*. Mahwah, NJ: Psychology Press.

Lu, D. 2006. "The Potential and Challenge of Remote Sensing-Based Biomass Estimation." *International Journal of Remote Sensing* 27 (7): 1297–1328. doi:10.1080/01431160500486732.

Maselli, F., G. Argenti, M. Chiesi, L. Angeli, and D. Papale. 2013. "Simulation of Grassland Productivity by the Combination of Ground and Satellite Data." *Agriculture, Ecosystems & Environment* 165 (0): 163–172. doi:10.1016/j.agee.2012.11.006.

Maselli, F., D. Papale, N. Puletti, G. Chirici, and P. Corona. 2009. "Combining Remote Sensing and Ancillary Data to Monitor the Gross Productivity of Water-Limited Forest Ecosystems." *Remote Sensing of Environment* 113 (3): 657–667. doi:10.1016/j.rse.2008.11.008.

McCallum, I., W. Wagner, C. Schmullius, A. Shvidenko, M. Obersteiner, S. Fritz, and S. Nilsson. 2009. "Satellite-Based Terrestrial Production Efficiency Modeling." *Carbon Balance and Management* 4 (1): 8. doi:10.1186/1750-0680-4-8.

Meroni, M., E. Marinho, N. Sghaier, M. Verstrate, and O. Leo. 2013. "Remote Sensing Based Yield Estimation in a Stochastic Framework — Case Study of Durum Wheat in Tunisia." *Remote Sensing* 5 (2): 539–557. doi:10.3390/rs5020539.

Meroni, M., F. Rembold, M. M. Verstraete, R. Gommes, A. Schucknecht, and G. Beye. 2014. "Investigating the Relationship between the Inter-Annual Variability of Satellite-Derived Vegetation Phenology and a Proxy of Biomass Production in the Sahel." *Remote Sensing* 6 (6): 5868–5884. doi:10.3390/rs6065868.

Meroni, M., M. M. Verstraete, F. Rembold, F. Urbano, and F. Kayitakire. 2014. "A Phenology-Based Method to Derive Biomass Production Anomalies for Food Security Monitoring in the Horn of Africa." *International Journal of Remote Sensing* 35 (7): 2472–2492. doi:10.1080/01431161.2014.883090.

Monteith, J. L., and C. J. Moss. 1977. "Climate and the Efficiency of Crop Production in Britain [and Discussion]." *Philosophical Transactions of the Royal Society of London. Series B, Biological Sciences* 281 (980): 277–294. doi:10.1098/rstb.1977.0140.

Mosnier, C., J. Agabriel, M. Lherm, and A. Reynaud. 2008. "Assessing Economic and Technical Impacts of Non Expected Weather Events on French Suckler Cow Farms Dynamics: A Dynamic

Recursive Farm Model." 12 Congress of the European Association of Agricultural Economists (EAAE), Ghent, August 26–29, 13.

Mosnier, C., S. Fourdin, J.-C. Moreau, A. Boutry, E. Le Floch, M. Lherm, and J. Devun. 2014. "Impacts des aléas climatiques en élevages bovin et ovin allaitants et demande de couverture assurantielle." *Notes et études socio-économiques, Centre d'études et de prospective* 38: 26.

Noury, J.-M., S. Fourdin, and Y. Pauthenet. 2013. "Livestock Farming Systems and Climate Change: Perception of Farmers and Adaptation Strategies." *Fourrages* 215: 211–219.

Piñeiro, G., M. Oesterheld, and J. Paruelo. 2006. "Seasonal Variation in Aboveground Production and Radiation-use Efficiency of Temperate rangelands Estimated through Remote Sensing." *Ecosystems* 9 (3): 357–373. doi:10.1007/s10021-005-0013-x.

Potter, C. S., J. T. Randerson, C. B. Field, P. A. Matson, P. M. Vitousek, H. A. Mooney, and S. A. Klooster. 1993. "Terrestrial Ecosystem Production: A Process Model Based on Global Satellite and Surface Data." *Global Biogeochemical Cycles* 7 (4): 811–841. doi:10.1029/93GB02725.

Pottier, E., A. Michaud, J. Farrié, S. Plantureux, and R. Baumont. 2012. "Les prairies permanentes françaises au cœur d'enjeux agricoles et environnementaux." *Innovations Agronomiques* 25: 85–97.

Quintana-Seguí, P., P. Le Moigne, Y. Durand, E. Martin, F. Habets, M. Baillon, C. Canellas, L. Franchisteguy, and S. Morel. 2008. "Analysis of Near-Surface Atmospheric Variables: Validation of the SAFRAN Analysis over France." *Journal of Applied Meteorology and Climatology* 47 (1): 92–107.

Rao, K. N. 2010. "Index Based Crop Insurance." *Agriculture and Agricultural Science Procedia* 1: 193–203. doi:10.1016/j.aaspro.2010.09.024.

Rembold, F., C. Atzberger, I. Savin, and O. Rojas. 2013. "Using Low Resolution Satellite Imagery for Yield Prediction and Yield Anomaly Detection." *Remote Sensing* 5 (4): 1704–1733. doi:10.3390/rs5041704.

Richardson, A. D., T. F. Keenan, M. Migliavacca, Y. Ryu, O. Sonnentag, and M. Toomey. 2013. "Climate Change, Phenology, and Phenological Control of Vegetation Feedbacks to the Climate System." *Agricultural and Forest Meteorology* 169: 156–173. doi:10.1016/j.agrformet.2012.09.012.

Risk Management Agency. 2013. *Rainfall and Vegetation Index Insurance Standards Handbook*, 53. Kansas City, MO: RMA.

Rodriguez, J. D., A. Perez, and J. A. Lozano. 2010. "Sensitivity Analysis of k-Fold Cross Validation in Prediction Error Estimation." *IEEE Transactions on Pattern Analysis and Machine Intelligence* 32 (3): 569–575. doi:10.1109/TPAMI.2009.187.

Roumiguié, A., A. Jacquin, G. Sigel, H. Poilvé, O. Hagolle, and J. Daydé. 2015. "Validation of a Forage Production Index (FPI) Derived from MODIS *f*Cover Time-Series Using High-Resolution Satellite Imagery: Methodology, Results and Opportunities." *Remote Sensing* 7 (9): 11525–11550. doi:10.3390/rs70911525.

Roumiguié, A., A. Jacquin, G. Sigel, H. Poilve, B. Lepoivre, and O. Hagolle. 2015. "Development of an Index-Based Insurance Product: Validation of a Forage Production Index Derived from Medium Spatial Resolution *F*cover Time Series." *GIScience & Remote Sensing* 52 (1): 94–113. doi:10.1080/15481603.2014.993010.

Rouse, J. W., R. H. Haas, J. A. Schell, and D. W. Deering. 1974. "Monitoring Vegetation Systems in the Great Plains with ERTS." Third Earth Resources Technology Satellite-1 Symposium, December 10–14, Washington, DC.

Royston, P. 1992. "Approximating the Shapiro-Wilk W-Test for Non-Normality." *Statistics and Computing* 2 (3): 117–119. doi:10.1007/BF01891203.

Ruget, F., R. Delécolle, C. Le Bas, M. Duru, N. Bonneviale, V. Rabaud, I. Donet, V. Pérarnaud, and S. Paniagua. 2001. "L'estimation régionale des productions fourrageres." In *Modélisation des agroécosystemes et aide à la décision*, 263–282. Montpellier: Cirad-Inra.

Ruget, F., S. Novak, and S. Granger. 2006. "Du modèle Stics au système Isop pour estimer la production fourragère. Adaptation à la prairie, application spatialisée." *Fourrages* 186: 241–256.

Running, S., D. Baldocchi, D. Turner, S. Gower, P. Bakwin, and K. Hibbard. 1999. "A Global Terrestrial Monitoring Network Integrating Tower Fluxes, Flask Sampling, Ecosystem Modeling and EOS

Satellite Data." *Remote Sensing of Environment* 70 (1): 108–127. doi:10.1016/S0034-4257(99)00061-9.

Running, S. W., R. R. Nemani, F. A. Heinsch, M. S. Zhao, M. Reeves, and H. Hashimoto. 2004. "A Continuous Satellite-Derived Measure of Global Terrestrial Primary Production." *Bioscience* 54 (6): 547–560. doi:10.1641/0006-3568(2004)054[0547:ACSMOG]2.0.CO;2.

Sandmark, T., J.-C. Debar, and C. Tatin-Jaleran. 2013. "The Emergence and Development of Agriculture Microinsurance." Discussion Paper, 86. Luxembourg: Microinsurance Network,.

Seaquist, J. W., L. Olsson, and J. Ardö. 2003. "A Remote Sensing-Based Primary Production Model for Grassland Biomes." *Ecological Modelling* 169 (1): 131–155. doi:10.1016/S0304-3800(03)00267-9.

Veroustraete, F., H. Sabbe, and H. Eerens. 2002. "Estimation of Carbon Mass Fluxes over Europe Using the C-Fix Model and Euroflux Data." *Remote Sensing of Environment* 83 (3): 376–399. doi:10.1016/S0034-4257(02)00043-3.

Veysset, P., D. Bebin, and M. Lherm. 2007. "Impacts de la sècheresse 2003 sur les résultats technico-économiques en élevage bovin allaitant charolais." *Fourrages* 191: 311–322.

Vidal, J.-P., E. Martin, L. Franchistéguy, M. Baillon, and J.-M. Soubeyroux. 2010. "A 50-Year High-Resolution Atmospheric Reanalysis over France with the Safran System." *International Journal of Climatology* 30 (11): 1627–1644. doi:10.1002/joc.v30:11.

Vrieling, A., M. Meroni, A. G. Mude, S. Chantarat, C. C. Ummenhofer, and K. de Bie. 2016. "Early Assessment of Seasonal Forage Availability for Mitigating the Impact of Drought on East African Pastoralists." *Remote Sensing of Environment* 174: 44–55. doi:10.1016/j.rse.2015.12.003.

Wang, Q., S. Adiku, J. Tenhunen, and A. Granier. 2005. "On the Relationship of NDVI with Leaf Area Index in a Deciduous Forest Site." *Remote Sensing of Environment* 94 (2): 244–255. doi:10.1016/j.rse.2004.10.006.

Xu, B., X. Yang, W. Tao, Z. Qin, H. Liu, and J. Miao. 2007. "Remote Sensing Monitoring upon the Grass Production in China." *Acta Ecologica Sinica* 27 (2): 405–413. doi:10.1016/S1872-2032(07)60012-2.

Yang, Y., H. Guan, S. Shang, D. Long, and C. T. Simmons. 2014. "Toward the Use of the MODIS ET Product to Estimate Terrestrial GPP for Nonforest Ecosystems." *IEEE Transactions on Geoscience and Remote Sensing* 11 (9): 1624–1628. doi:10.1109/LGRS.2014.2302796.